Neurobiology of Disease

Developmental Shift of Cyclophilin D Contribution to Hypoxic-Ischemic Brain Injury

Xiaoyang Wang,[1,4] Ylva Carlsson,[1,7]* Emy Basso,[5]* Changlian Zhu,[2,4] Catherine I. Rousset,[1,8] Andrea Rasola,[5] Bengt R. Johansson,[3] Klas Blomgren,[2] Carina Mallard,[1] Paolo Bernardi,[5] Michael A. Forte,[6] and Henrik Hagberg[1,7,8]

[1]Perinatal Center and [2]Center for Brain Repair and Rehabilitation, Institute of Neuroscience and Physiology, and [3]The Electron Microscopy Unit, Institute for Biomedicine, University of Gothenburg, SE-405 30 Gothenburg, Sweden, [4]Department of Pediatrics, The Third Affiliated Hospital of Zhengzhou University, 450052 Zhengzhou, China, [5]Consiglio Nazionale delle Ricerche, Institute of Neuroscience and Department of Biomedical Sciences, University of Padova, 35121 Padova, Italy, [6]Vollum Institute, Oregon Health & Science University, Portland, Oregon 97239, [7]Perinatal Center, Department of Obstetrics and Gynecology, Sahlgrenska Academy, SE-416 84 Gothenburg, Sweden, and [8]Institute of Reproductive and Developmental Biology, Imperial College, London W12 0NN, United Kingdom

Cyclophilin D (CypD), a regulator of the mitochondrial membrane permeability transition pore (PTP), enhances Ca^{2+}-induced mitochondrial permeabilization and cell death in the brain. However, the role of CypD in hypoxic-ischemic (HI) brain injury at different developmental ages is unknown. At postnatal day (P) 9 or P60, littermates of CypD-deficient [knock-out (KO)], wild-type (WT), and heterozygous mice were subjected to HI, and brain injury was evaluated 7 d after HI. CypD deficiency resulted in a significant reduction of HI brain injury at P60 but worsened injury at P9. After HI, caspase-dependent and -independent cell death pathways were more induced in P9 CypD KO mice than in WT controls, and apoptotic activation was minimal at P60. The PTP had a considerably higher induction threshold and lower sensitivity to cyclosporin A in neonatal versus adult mice. On the contrary, Bax inhibition markedly reduced caspase activation and brain injury in immature mice but was ineffective in the adult brain. Our findings suggest that CypD/PTP is critical for the development of brain injury in the adult, whereas Bax-dependent mechanisms prevail in the immature brain. The role of CypD in HI shifts from a predominantly prosurvival protein in the immature to a cell death mediator in the adult brain.

Key words: brain injury; hypoxia-ischemia; mitochondria; development; cyclophilin D; cell death

Introduction

The mechanisms underlying cell damage and the ensuing cell death after hypoxia-ischemia (HI) of the brain remain unclear. Mitochondrial permeabilization (MP) plays an important role as an event that marks the point of no return in multiple pathways to cell death through at least two alternative routes. The first relies on the opening of the permeability transition pore (PTP) in the inner mitochondrial membrane, a process enhanced by cyclophilin D (CypD) and prevented by the CypD inhibitor cyclosporine A (CsA); the second involves proapoptotic members of the Bcl-2 protein family and is thought to be independent of the PTP, often based on the lack of inhibition by CsA. Both mechanisms, which are not mutually exclusive, are involved in the ensuing release of apoptogenic proteins from mitochondria (Scorrano et al., 1997; Zamzami et al., 2005; Zoratti et al., 2005; Bernardi et al., 2006). However, the exact role of and interaction between these mechanisms in neuronal cell death in response to HI is debated. It has been shown previously that HI in the immature brain induces MP (Puka-Sundvall et al., 2001) with the release of proapoptotic proteins (Wang et al., 2004b), leading to the initiation of both caspase-dependent (Wang et al., 2001) and apoptosis-inducing factor (AIF)-dependent cell death (Zhu et al., 2003). However, and contrary to the situation in the adult brain (Uchino et al., 1995; Matsumoto et al., 1999), CsA fails to protect the neonatal brain after HI (Puka-Sundvall et al., 2001). This finding suggests that PTP-mediated MP is not involved in HI injury in the immature brain. Alternatively, CsA, which requires P-glycoprotein-mediated active uptake into the CNS (Sakata et al., 1994), is not transferred across the immature blood–brain barrier to the same extent as in the adult. Significant alterations in Bcl-2 family protein expression after neonatal HI have also been noted (Northington et al., 2001), and the proapoptotic versus antiapoptotic Bcl-2 family protein balance seems critical for the development of neonatal HI injury (Parsadanian et al., 1998; Gibson et al., 2001; Hallin et al., 2006; Ness et al., 2006). CypD, a regulator of the PTP, is important in necrotic cell death triggered by ischemia/reperfusion injury in the adult brain (Khaspekov et al., 1999; Schinzel et al., 2005; Rasola and Bernardi, 2007), whereas the role of the
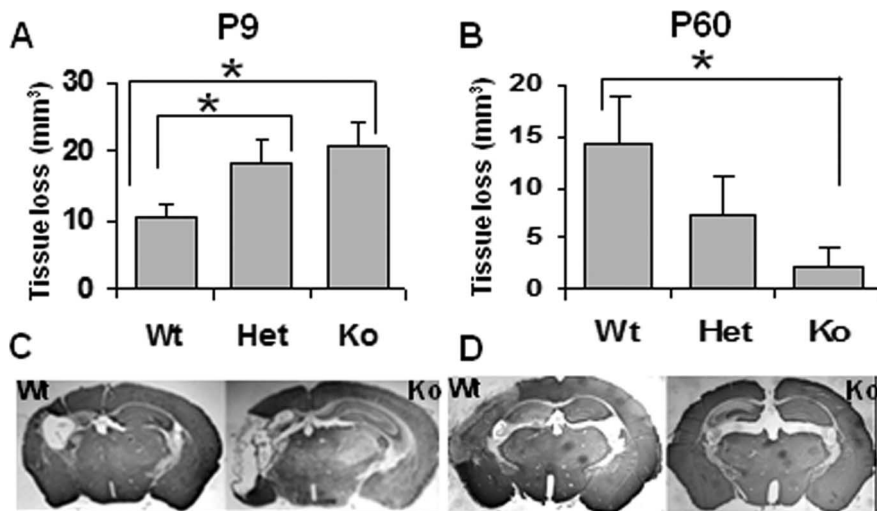
Figure 1. Effect of CypD deficiency on HI injury in neonatal (P9) and adult (P60) mice. Volume of brain total tissue loss in P9 (***A***) and P60 (***B***) mice. Representative photomicrographs of MAP2-stained sections of P9 (***C***) and P60 (***D***) mouse brains. P9 mice: WT, $n = 16$; Het, $n = 40$; KO, $n = 19$. P60 mice: WT, $n = 18$; Het, $n = 28$; KO, $n = 13$. *$p < 0.05$.

CypD-regulated PTP in HI injury of the immature brain is still unclear. The aim of this study was to examine a possible protective role of CypD ablation and the relative contributions of mitochondrial dysfunction, opening of the PTP, and the proapoptotic Bcl-2 family protein Bax in HI brain damage in early postnatal life, an issue with important implications for human perinatal brain diseases.

Materials and Methods

Animals. Wild-type (WT) (C67BL/6J) and CypD knock-out (KO) mice were originally from Oregon Health and Sciences University (Portland, OR). Littermate animals with mixed genotypes, including CypD homozygous, heterozygous mutant (Het), and WT mice, were used for experiments. All mice were housed with a 12 h light/dark cycle. *Ad libitum* access to a standard laboratory chow diet (B & K, Solna, Sweden) and drinking water was provided. All animal experimentation was approved by the Ethical Committee of Gothenburg University (ethical number 314-2005, 269-2006).

Genotyping. The genotype of mice was determined by PCR of genomic DNA obtained from mouse tails according to a method described previously (Wang et al., 2006). The WT allele was detected using a forward primer (5′-GCA TCG ATG CGA CAG CGA TGC TAG CGC TGC-3′) and a reverse primer (5′-ATT CCC TGT GTC TCC TCT TAG-3′). To detect the mutant allele, a forward primer (5′-GCT ATC GTG GCT GGC CAC GAC G-3′) and a reverse primer (5′-GGC GAT ACC GTA AAG CAC GAC G-3′) were used. CypD KO mice were identified by the presence of a single 550 bp DNA band. WT mice were identified by a single 540 bp product. Het mice were identified by the presence of both bands.

HI procedure. At postnatal day (P) 9 or P60, littermates of CypD KO, WT, and Het of both genders were anesthetized with halothane (3.0% for induction and 1.0–1.5% for maintenance) in a mixture of nitrous oxide and oxygen (1:1). The left common carotid was ligated with prolene sutures. Mice were returned to the cage and allowed to recover for 1 h and were subsequently placed in an incubator perfused with a humidified gas mixture (10.00 ± 0.01% oxygen in nitrogen) at 36°C for 40 min (P9) or 30 min (P60) to acquire a similar extent of injury (Vannucci et al., 2001; Zhu et al., 2005). After hypoxic exposure, the pups were returned to their dam until they were killed. Different hypoxia times were chosen based on the fact that animals have different reactions to this HI model according to their age, as shown previously (Vannucci et al., 2001; Zhu et al., 2005; Lafemina et al., 2006). Therefore, the duration of hypoxia must be varied for individual ages to achieve an adequate, consistent degree of brain damage with minimal mortality. Sham surgery (5 min of anesthesia and cervical incision and suture) did not present significant differences compared with naive controls with respect to energy and glycolytic metabolites in the brain, acid base/blood gas status (our unpublished data), expression of immediate early genes (Gubits et al., 1993), and apoptosis (Grafe, 1994); therefore, we used naive controls without sham surgery as normal controls in the present study.

Assessment of brain damage. Seven days after HI, mice were deeply anesthetized and perfusion fixed with 5% formaldehyde in 0.1 M PBS. The brains were rapidly removed and immersion fixed in 5% formaldehyde at 4°C for 24 h. After dehydration with graded ethanol and xylene, the brains were paraffin embedded and cut into 6 μm frontal sections. Every 100th section was stained for microtubule-associated protein-2 (MAP2) (clone HM-2, 1:2000; Sigma), and volumes of total tissue loss in different brain regions were evaluated as described previously (Wang et al., 2004a,b) by a person unaware of the HI groups. Briefly, areas displaying loss of MAP2 staining were measured using Micro Image (Olympus), and the volumes were calculated according to the Cavalieri Principle using the following formula: $V = SA \times p \times T$, where V is the total volume, SA is the sum of the areas measured, p is the inverse of the sections sampling fraction, and T is the section thickness. Total tissue loss was calculated by subtracting the MAP2-positive volume of the ipsilateral hemisphere from the contralateral hemisphere.

Sample preparation for caspase activity assays and immunoblotting. Mice were killed at 1.5, 3, 6, or 24 h after HI ($n = 6$ per group). Control animals were killed on P3, P9, P21, or P60 ($n = 6$ per age). The brains were rapidly dissected out on a bed of ice. Ice-cold isolation buffer was added [15 mM Tris-HCl, pH 7.6, 320 mM sucrose, 1 mM DTT, 1 mM MgCl$_2$, 3 mM EDTA-K, and 0.5% protease inhibitor mixture (P8340; Sigma)], and homogenization was performed gently by hand (to preserve mitochondrial integrity) in a 2 ml glass/glass homogenizer (VWR International). The mitochondrial, cytosolic, and nuclear fractions were separated according to a method described previously (Wang et al., 2003). Briefly, the homogenates were centrifuged at 800 × g at 4°C for 10 min. The pellets were washed in homogenizing buffer and recentrifuged, producing a crude nuclear pellet (P$_1$). The supernatant was further centrifuged at 9200 × g for 15 min at 4°C, producing a crude mitochondrial fraction in the pellet (P$_2$) and a cytosolic fraction in the supernatant (S). All fractions were stored at − 80°C. S fractions were used for caspase assays. P$_2$ and S fractions were used for immunoblotting.

Caspase activity assays. Caspase activity was measured as described previously (Wang et al., 2001). Briefly, cleavage of Ac-DEVD-AMC [acetyl-Asp-Glu-Val-Asp-(4-methyl-coumaryl-7-amide)] (for caspase-3-like activity; Peptide Institute), Ac-VDVAD-AFC (acetyl-Val-Asp-Val-Ala-Asp-7-amino-4-trifluoromethylcoumarin) (for caspase-2), and Ac-LEHD-AFC (acetyl-Leu-Glu-His-Asp-7-amino-4-trifluoromethyl-coumarin) (for caspase-9) (Enzyme Systems Products) was measured at 37°C using the SpectraMax Gemini Microplate Spectrofluorometer (Molecular Devices) with the appropriate excitation and emission wavelengths (excitation wavelength 380 nm and emission wavelength 460 nm for caspase-3; excitation wavelength 400 nm and emission wavelength 505 nm for caspase-2 and caspase-9) and expressed as picomoles 7-amino-4-methylcoumarin (for caspase-3) or 7-amino-4-trifluoromethylcoumarin (for caspase-2 and caspase-9) released per milligram of protein and minute.

Immunoblotting. Immunoblotting was performed as described previously (Wang et al., 2003). Briefly, after blocking with 30 mmol/L Tris-HCl, pH 7.5, 100 mmol/L NaCl, and 0.1% Tween 20 containing 5% fat-free milk powder for 1 h at room temperature, the membranes were incubated with primary antibodies: adenine nucleotide translocase (N-19, sc-9299), AIF (D-20, sc-9416), and Bax (N-20, sc-493) (all from Santa Cruz Biotechnology), CypD (PA1–028; AH Bioreagents), actin (A2066;
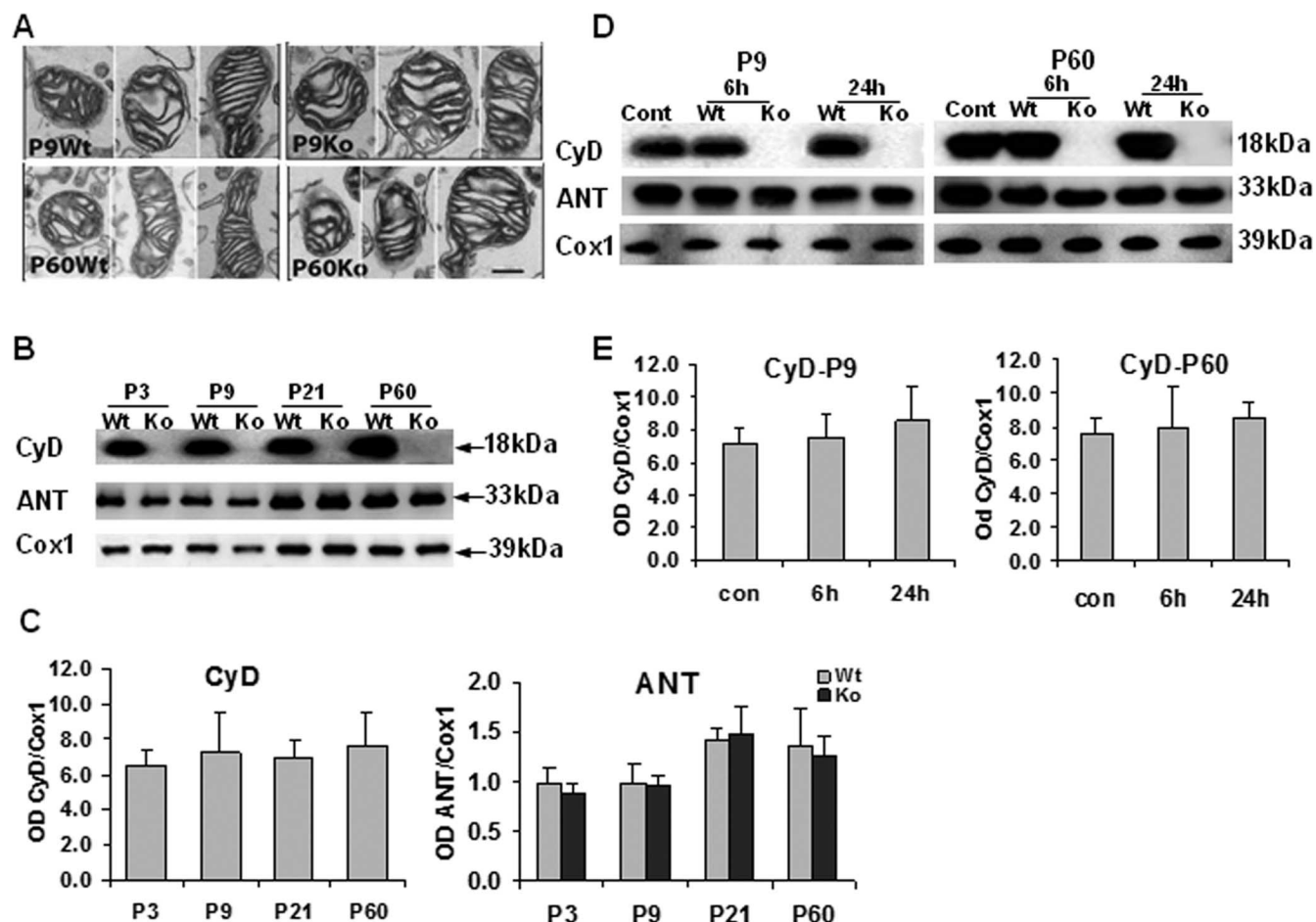
Figure 2. Brain mitochondria morphology and PTP-relevant molecular expression in WT and CypD KO neonatal (P9) versus adult (P60) mice. ***A***, Electron microscopy; morphology of isolated control brain mitochondria in WT versus KO mice at P9 and P60. $n = 2$ per group. Scale bar, 200 nm. ***B–E***, Representative immunoblotting pictures (***B***, ***D***) and immunoblotting quantification (***C***, ***E***) of mitochondrial CypD (CyD), and ANT expression in WT and KO mice at P3, P9, P21, and P60 (***B***, ***C***), as well as 6 and 24 h after HI in the ipsilateral hemispheres (***D***, ***E***). $n = 6$ per group. The mitochondrial marker Cox1 was used as protein loading control. Cont, Normal control brains from WT mice; OD, optical density.

Sigma), cytochrome oxidase 1 (Cox1) (A21344; Invitrogen), and cytochrome c (cyt c) (556433; BD PharMingen) at room temperature for 1 h, followed by an appropriate peroxidase-labeled, secondary antibody (Vector Laboratories) for 30 min at room temperature. Immunoreactive species were visualized using the Super Signal Western Dura substrate (Pierce) and an LAS 1000-cooled CCD camera (Fujifilm). Immunoreactive bands were quantified using the Image Gauge software (Fujifilm).

Immunohistochemistry and immunofluorescence staining. Mice were killed at 6 or 24 h after HI ($n = 6$ per group). These time points were chosen because our previous work (Zhu et al., 2003, 2005) has shown that immunohistochemical expression of AIF, cyt c, and caspase-3 was increased at these time points. Immunohistochemistry and immunofluorescence stainings were performed as described previously (Wang et al., 2003). Briefly, nonspecific binding was blocked for 30 min with 4% horse, goat, or donkey serum (depending on the species used to raise the secondary antibody) in PBS. The following primary antibodies were used: anti-AIF (1:1000, D-20, sc-9416; Santa Cruz Biotechnology), cyt c (1:500, 556433; BD PharMingen), and MAP2 (1:2000). After incubating the primary antibodies for 1 h at room temperature, the appropriate, biotinylated secondary antibodies (all from Vector Laboratories) were added for 1 h at room temperature. Visualization was performed using Vectastain ABC Elite with 0.5 mg/ml 3,3′-diaminobenzidine enhanced with 15 mg/ml ammonium nickel sulfate, 2 mg/ml β-D-glucose, 0.4 mg/ml ammonium chloride, and 0.01 mg/ml β-glucose oxidase (all from Sigma). For the immunofluorescence staining, primary antibodies used were as follows: cyt c and anti-active forms of caspase-3 (1:100, 557035; BD PharMingen) or AIF (1:1000). Secondary antibodies used were don-

key anti-mouse 488 (green, 1:500) and donkey anti-rabbit 546 (red, 1:500), and sections were mounted with 4′, 6′-diamidino-2-phenylindole (DAPI) (Invitrogen) medium. Sections were analyzed under an Olympus BX60 fluorescence microscope equipped with an Olympus DP50 cooled digital camera, and images were collected and processed using Olympus Micro Image (version 4.0).

Electron microscopy. Brain mitochondria were isolated from normal WT and CypD KO mice of P9 and P60 ($n = 2$ per group) according to the method described above (see Sample preparation for caspase activity assays and immunoblotting) and were fixed with a mixture of 2% paraformaldehyde, 2.5% glutaraldehyde, and 0.02% sodium azide in 0.05 M sodium cacodylate, embedded in epoxy resin (Agar 100), sectioned and stained with lead citrate and uranyl acetate, and examined with a Zeiss 912AB electron microscope equipped with a MegaView III camera (Soft Imaging Systems) for digital image capture.

Measurement of mitochondrial Ca^{2+} uptake. Mitochondria were isolated by centrifugation at $2000 \times g$ for 3 min; the supernatant was centrifuged at $12,000 \times g$ for 6 min. After washing, the resulting pellet was resuspended in isolation buffer (in mM: 225 mannitol, 75 sucrose, and 5 HEPES, pH 7.4). The Ca^{2+} retention capacity (CRC) of mitochondrial preparations was assessed fluorimetrically in the presence of the Ca^{2+} indicator Calcium Green-5N (Invitrogen) with a PerkinElmer Life Sciences LS50B spectrofluorimeter exactly as described previously (Fontaine et al., 1998) (see figure legends). The instruments were equipped with magnetic stirring and thermostatic control. The incubation conditions are specified in the figure legends.

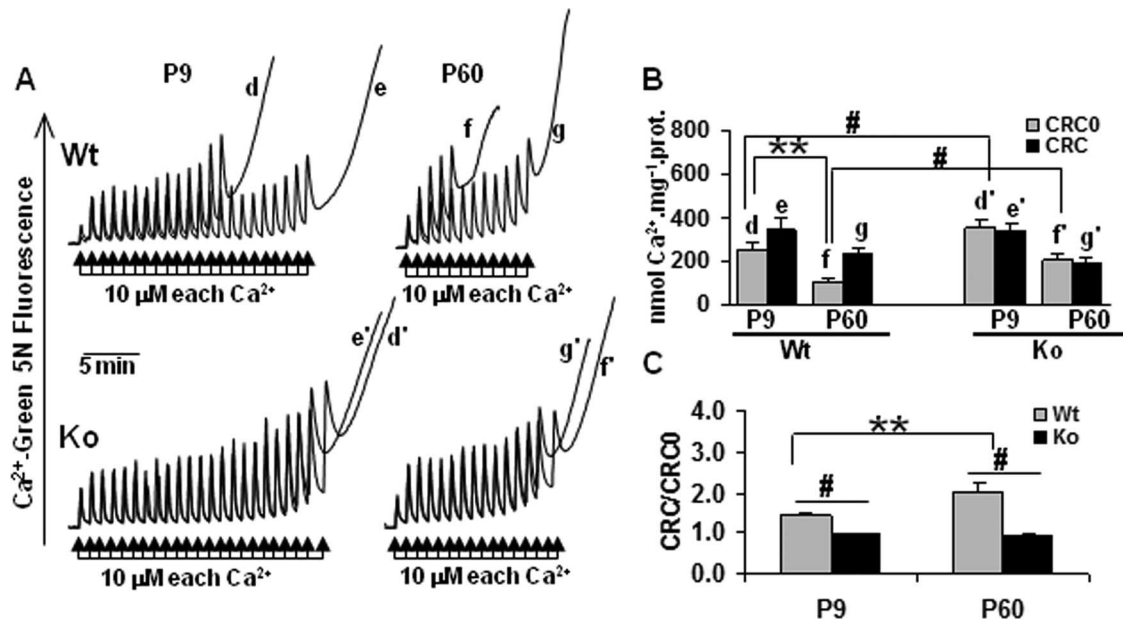*Bax inhibition experiments.* Five microliters of Bax-inhibiting peptide

Figure 3. CRC of WT and CypD KO mouse brain mitochondria in neonatal P9 and adult P60 mice. Effect of CsA. ***A***, The incubation medium contained 120 mM KCl, 10 mM Tris–3-(N-morpholino)-propanesulfonic acid, 5 mM glutamate-Tris, 2.5 mM malate-Tris, 1 mM Pi-Tris, 20 μM EGTA-Tris, and 1 μM Calcium Green-5N, pH 7.4. The experiments were started by the addition of 1 mg of mitochondria from WT (traces ***d – g***) or KO (traces ***d′ – g′***) mice, followed 1 min later by the indicated concentrations of Ca^{2+} (arrows); in the experiments of traces ***e***, ***e′***, ***g***, and ***g′***, 0.8 μM CsA was added before adding mitochondria. Traces shown are representative of at least four experiments. ***B***, Quantitative assessment of the mitochondrial CRC. Error bars refer to SEM of at least four replicate experiments per condition. ***C***, Ratio between the CRC detected in the presence (CRC) and absence (CRC0) of 0.8 μM CsA. **$p < 0.01$, compared between neonatal WT and adult WT mice; #$p < 0.05$, compared between WT and KO of the same age.

(BIP) V5 (5 mg/ml; catalog #196810; Calbiochem) or BIP negative control (BIPN) (5 mg/ml; catalog #196811; Calbiochem) dissolved in saline was intracerebroventricularly injected immediately before hypoxia ($n = 6$ in each group) according to a method described previously (Zhu et al., 2003) using a syringe attached to a microinjection pump (CMA) at a speed of 1 μl/min. In pilot experiments, injections of blue dye were performed to find the appropriate location. Mice were killed at 24 h after HI, i.e., a time when most commonly used apoptosis markers including caspase-3 activation reach a maximum level in this model. The gross morphology brain injury score was evaluated according to a method modified from the original description by Yager et al. (1992), which has been found to correlate well with tissue volume loss (Wang et al., 2004a). Briefly, after dissecting out the brain, the degree of injury was evaluated by inspection of the brain surface according to the following scale: grade 0, normal, equal size of the two hemispheres and no visible white lesion; grade 1, a small white lesion; grade 2, hypotrophy and large cysts in the ipsilateral hemisphere; grade 3, only parasagittal brain tissue remains in the ipsilateral hemisphere; and grade 4, total loss of the ipsilateral hemisphere. Cytosolic cell fractions were separated as described above (see Sample preparation for caspase activity assays and immunoblotting) and stored at −80°C for caspase-3 analysis.

Determination of cyt c *release from isolated brain mitochondria.* Brain mitochondria were isolated according to the method described above (see Sample preparation for caspase activity assays and immunoblotting). The Bcl-2 homology 3 (BH3) peptide [with the sequence 53DAST-KKLSECLKRIGDELDSNME LQRMIAAVDTD86, as described previously (Polster et al., 2003)] and the control BH3 peptide that had identical sequences except for a single substitution of arginine for glycine at position 67 (BH3 G67R) were synthesized by Sigma. Full-length recombinant Bax was from Abnova (H00000581-P01). According to a method described previously (Polster et al., 2003), isolated mouse brain mitochondria (0.5–1 mg/ml final concentration) were suspended in 0.25 ml of KCl assay medium supplemented with 4 mM MgCl$_2$, 3 mM ATP, 0.8 mM ADP, 250 μM EGTA, 5 mM succinate, and 2 μM rotenone and incubated at 30°C. Bax (100 nM) or vehicle control for Bax was also included when indicated. BH3 peptide or control BH3 peptide (each at 60 μM) was added after 2 min of incubation. At 16 min after the addition of BH3

peptide or vehicle control, mitochondria were pelleted by centrifugation at 13,400 × g for 5 min. For quantitative comparisons, the release of cyt c in the supernatant was assayed using an ELISA kit (MCTC0; R & D Systems) according to the instructions of the manufacturer.

Statistics. The Student's *t* test was used when comparing two groups, whereas ANOVA followed by Fisher's PLSD *post hoc* test was used when comparing three or more groups. The Mann–Whitney test was used to compare gross morphology. $p < 0.05$ was considered statistically significant. All data are expressed as mean ± SEM.

Results
Effects of CypD deficiency on HI brain injury in neonatal versus adult mice
Analysis of brain injury in P9 WT, CypD KO, and Het mice revealed a more pronounced damage in CypD KO mice (total tissue loss, 20.6 ± 3.5 mm^3; $n = 19$) than in WT mice (10.5 ± 1.7 mm^3; $n = 16$; $p = 0.017$) 7 d after HI (Fig. 1*A*,*C*). On the contrary, and in keeping with a previous study (Schinzel et al., 2005), absence of CypD resulted in a significant decrease in HI brain injury at P60. The total tissue loss in P60 mice was 2.3 ± 1.9 mm^3 in KO ($n = 13$) versus 14.3 ± 4.8 mm^3 in WT mice ($n = 18$; $p = 0.035$) (Fig. 1*B*,*D*). Although brain injury and apoptosis in the immature brain has been shown previously to depend on gender (Du et al., 2004; Hagberg et al., 2004; Hurn et al., 2005; Zhu et al., 2006; Johnston and Hagberg, 2007; Nijboer et al., 2007; Renolleau et al., 2007, 2008), subanalysis according to sex demonstrated that the influence of CypD deficiency on brain injury in immature and adult mice did not depend on gender in our protocols (data not shown).

Effect of CypD deficiency on brain mitochondrial morphology and PTP function in neonatal versus adult mice
To investigate whether the CypD genotype differentially affected mitochondrial ultrastructure at the two ages, EM on brain

mitochondria-enriched cell fractions was performed. No obvious differences in mitochondrial morphology between WT and KO mice at P9 or P60 were revealed (Fig. 2A). CypD was as abundant in immature as in mature brain mitochondria with the development from P3 to P60 ($p > 0.05$) (Fig. 2B,C). ANT, a putative PTP regulator (Kokoszka et al., 2004), over the Cox1 were expressed at slightly higher levels in mature brains (compare P21 and P60 with P3 and P9) (Fig. 2B,C), but the increases were not statistically significant ($p > 0.05$). Neither CypD ablation nor HI influenced the expression of ANT, and HI did not alter the expression of CypD itself in the mitochondria-enriched cell fractions ($p > 0.05$) (Fig. 2D,E). The functional properties of the PTP were evaluated in brain mitochondria prepared from P9 and P60 WT and KO mice. The CRC assay measures the threshold amount of Ca^{2+} required to open the PTP in isolated mitochondria. As expected (Basso et al., 2005), brain mitochondria from both neonatal and adult KO mice were desensitized to Ca^{2+}, requiring approximately twice the amount of Ca^{2+} to open the PTP than mitochondria from WT animals (Fig. 3A,B, compare traces d and d', f and f'). Interestingly, brain mitochondria from neonatal WT mice required far more Ca^{2+} to open the PTP than mitochondria from adult mice (Fig. 3A, compare traces d and f), regardless of the presence of CypD (Fig. 3A, compare traces d', f'). CsA was a more efficient desensitizer in adult than in neonatal WT mitochondria, whereas it was ineffective in mitochondria from KO animals, as expected (Fig. 3B,C).

Effect of CypD deficiency on apoptotic mechanisms after HI in neonatal versus adult mice

Caspase-2, caspase-3, and caspase-9 were markedly induced in the brain after HI at P9, whereas the activation and alterations were negligible at P60 (Fig. 4A–C), similar to previous reports showing that there is a significant decrease in caspase activation with age (Cheng et al., 1997; Hu et al., 2000; Wang et al., 2001; Zhu et al., 2005). At P9, caspase-2, caspase-3, and caspase-9 were all significantly more activated in KO than WT mice (Fig. 4A–C, left), whereas at P60 the opposite was observed (Fig. 4A–C, right). A decrease of cyt c was observed in the mitochondrial fraction, matched by an increase in the cytosolic fraction after HI at both ages. At P9, the release of cyt c at 24 h after HI was much more pronounced in KO compared with WT mice, whereas in adult mice, the opposite occurred (Fig. 5A,D,E). AIF decreased at 6 and 24 h after HI in the mitochondria-enriched cell fractions in both WT and KO mice at P9, but the loss was most pronounced at 24 h after HI in KO mice (Fig. 5A,B). AIF changes after HI in the adult brain were limited and independent of genotype (Fig. 5A,C). In P9 KO mice, post-HI changes were further confirmed by immunohistochemistry (Fig. 5F). AIF immunoreactivity translocated from mitochondria to nuclei after HI (Fig. 5F, a–h). Double immunostaining showed that cyt c expression shifted from a weak expression in the cytosol of normal control brain cells to a much stronger staining with a diffuse cytosolic localization in cells that highly expressed the cleaved active form of caspase-3 after HI (Fig. 5F, i–p).

Effect of CypD deficiency on Bax expression and the role of Bax inhibition in HI brain injury in neonatal versus adult mice

We next investigated the role of Bax-mediated mechanisms in HI brain injury at the two ages. In normal control brains from the WT mice, a marked decrease of mitochondrial Bax expression independent of CypD during the development from P3 to P60 was noticed (Fig. 6A). After HI at P9, translocation of Bax to
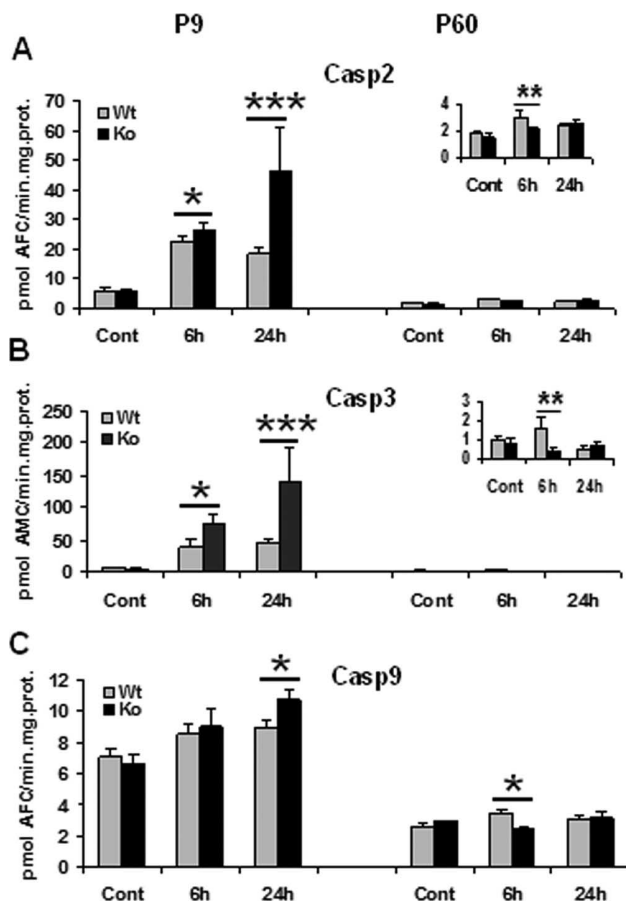

Figure 4. Effect of CypD deficiency on apoptosis after HI in neonatal (P9) and adult (P60) mice. Caspase-2 (**A**), caspase-3 (**B**), and caspase-9 (**C**) activation at 6 and 24 h after HI in P9 (left column) and P60 (right column) mice in ipsilateral hemispheres. Cont, Normal control brains without any treatment. *$p < 0.05$, **$p < 0.01$, ***$p < 0.001$, compared between WT and KO at the same time point.

mitochondria increased at 1.5 and 3 h in both genotypes, but the increase was more pronounced in KO than in WT individuals at 3 h (Fig. 6B). In brains of P60 mice, Bax expression was rather low and no obvious changes after HI were detected (data not shown). To further investigate the role of Bax in HI brain injury, a single injection of BIP was administered intracerebroventricularly immediately before HI in the WT mice. BIP reduced brain injury by 79% (brain injury score, 0.3 ± 0.05 in BIP group vs 1.4 ± 0.2 in BIPN group) and caspase-3 activation by 65% (Fig. 6C) in P9 WT mice, whereas the corresponding effects were negligible in P60 WT mice on both the brain injury (brain injury score, 2.8 ± 0.15 in BIP group vs 3.0 ± 0.2 in BIPN group) and caspase-3 activation (Fig. 6D). In addition, cyt c release was assessed *in vitro* by adding BH3 peptide to isolated brain mitochondria in a cytosol-like medium. Under these conditions, BH3 peptide induced cyt c release in both the absence and presence of exogenous full-length recombinant Bax at P9 (Fig. 7, top), whereas at P60, BH3 peptide-induced cyt c release required the presence of exogenous Bax (Fig. 7, bottom), as reported previously (Polster et al., 2003), probably because the endogenous level of Bax in adult brain mitochondria was too low (Fig. 6A). Moreover, BH3 peptide induced a more pronounced cyt c release in KO than in WT mice in P9 brain mitochondria (Fig. 7A). In contrast, BH3-induced cyt c release was attenuated in mitochondria from KO compared with WT mice at P60 (Fig. 7B). Bax alone did not elicit cyt c release from
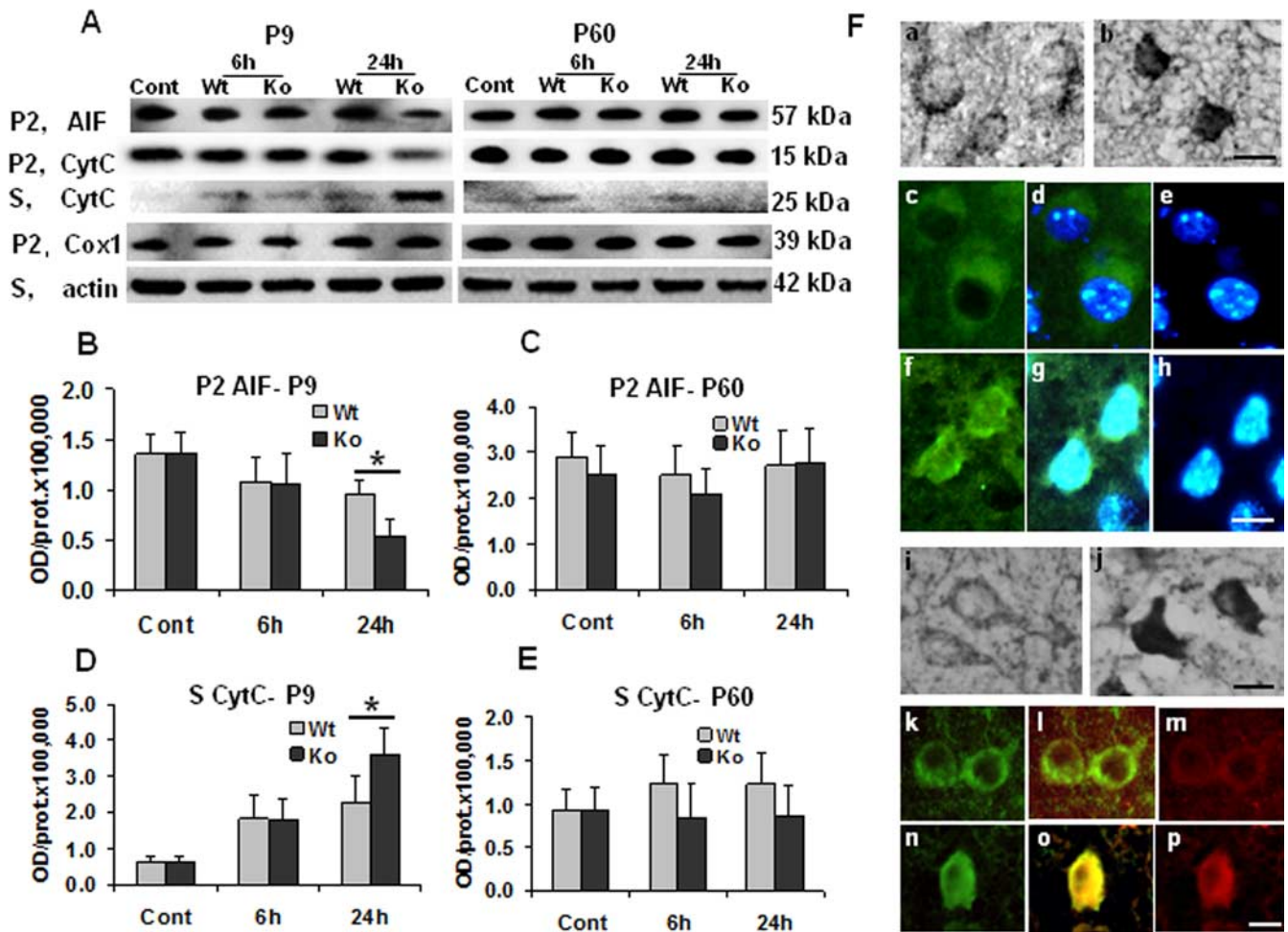
Figure 5. Effect of CypD deficiency on mitochondrial proapoptotic protein release after HI in neonatal (P9) and adult (P60) mice. *A*, Representative immunoblotting pictures show AIF and cyt *c* release from mitochondria 6 and 24 h after HI in ipsilateral hemispheres. 6h, 24h, Six or 24 h after HI; Cont, normal control brains from WT mice. *B, C,* Quantification of immunoblotting for AIF in the mitochondria-enriched cell fractions (P_2) at P9 and P60. *D, E,* Quantification of immunoblotting for cyt *c* in the cytosolic cell fractions (S) at P9 and P60. *$p < 0.05$. *F,* Representative pictures of AIF and cyt *c* immunostaining in CypD KO mouse brains at P9. AIF in a normal control brain (*a, c, d*) and 24 h after HI (*b, f, g*). cyt *c* in a normal control brain (*i, k, l*) and 24 h after HI (*j, n, o*). Note the more condensed apoptotic phenotype of the nuclei in *h. c, f,* AIF staining; *e, h,* DAPI nuclei staining; *d, g,* merged pictures of AIF (green) and DAPI (blue); *k, n,* cyt *c* staining; *m, p,* caspase-3 staining; *l, o,* merged pictures of cyt *c* (green) and caspase-3 (red). Scale bars, 10 μm.

isolated P9 brain mitochondria, but exogenous Bax enhanced the effect of the BH3 peptide (Fig. 7*A*).

Discussion

In neurons, MP appears to be a critical event in response to HI in both the immature and the adult brain. MP triggers the release of apoptotic factors such as cyt *c* and AIF, proteins contributing to the propagation of the apoptotic cascade and the execution of cell death. However, the mechanism leading to MP after HI is controversial and may depend on brain maturity. The present data show that a CypD-dependent PTP is critical for the development of HI injury in the adult brain but not so important in the neonatal brain in which Bax-dependent MP is instead essential. Moreover, CypD prevents rather than enhances MP in the immature brain, because lack of CypD worsens injury (Fig. 8). We propose that these age-dependent differences in mitochondrial responses to injury are of fundamental importance not only for mechanistic reasons but also for the selection of a neuroprotective strategy in the neonate.

CypD KO mice exhibit a normal phenotype and brain morphology, including normal cerebrovasculature (Basso et al., 2005; Schinzel et al., 2005). Confirming this, we found an unaltered

brain mitochondrial morphology in CypD-deficient mice. Given the critical role of apoptosis during embryogenesis, these data suggest that CypD is not essential for physiological apoptosis in the early stages of development. Furthermore, various cells isolated from CypD KO mice undergo apoptosis normally in response to various stimuli, including Bax activation (Baines et al., 2005; Nakagawa et al., 2005). Several studies have revealed CypD to be an important PTP regulator critical for Ca^{2+}-mediated, CsA-inhibited MP induction and necrosis (for review, see Rasola and Bernardi, 2007). In the present study, we found that the lack of CypD conferred dramatic protection against HI-induced brain injury in adult mice, which agrees with a pivotal role of the CypD-dependent PTP in adult ischemic stroke (Schinzel et al., 2005). Caspase activation after HI in P60 animals remained relatively low with the caspase-3 target α-fodrin not being cleaved (data not shown), suggesting that CypD-dependent, apoptosis-independent processes are of central importance in oxidative stress-induced cell death in the adult (Baines et al., 2005; Nakagawa et al., 2005). In contrast, the apoptotic cascade is thought to play a major role in neonatal HI-induced brain injury (Cheng et al., 1997; Hu et al., 2000; Zhu et al., 2005). In our study, CypD
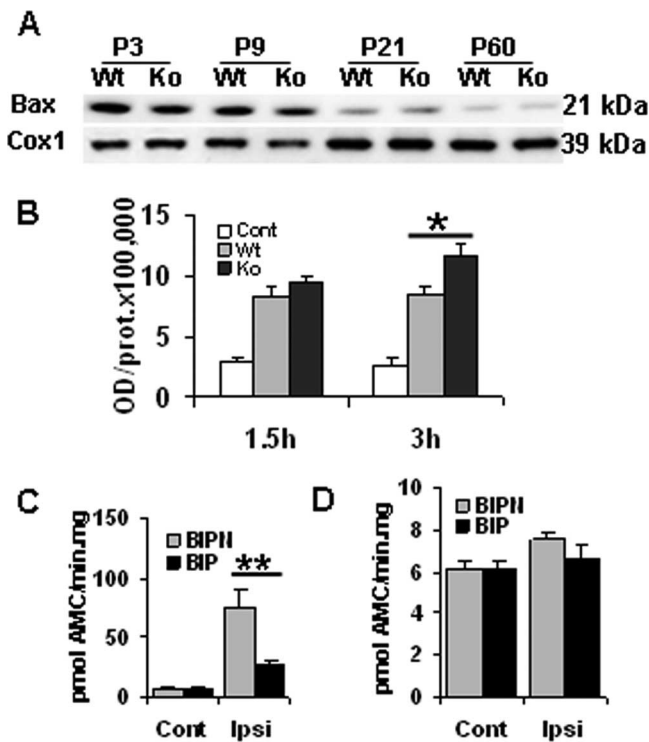
Figure 6. Bax expression during development and after HI in WT and CypD KO mice brain mitochondria in neonatal (P9) and adult (P60) mice. ***A***, Representative immunoblotting pictures of Bax expression at P3, P9, P21, and P60. ***B***, Quantification of immunoblotting for Bax in mitochondria-enriched cell fractions after HI at P9. Cont, Normal control brain from P9 WT mice. ***C***, ***D***, Effect of Bax inhibition in neonatal and adult brain injury in WT mice. Caspase-3 activation 24 h after HI in P9 (***C***) and P60 (***D***) WT mouse brains. Cont, Normal control brains from WT mice; Ipsi, ipsilateral hemisphere. $*p < 0.05$; $**p < 0.01$.

Figure 7. BH3 peptide induced the release of cyt c from isolated brain mitochondria of WT and CypD KO mice in neonates (P9, top) and adults (P60, bottom), measured by ELISA. Cont, Control peptide; Veh, vehicle control for Bax [50 mM Tris-HCl and 10 mM reduced glutathione (L-form), pH 8.0]; Bax, full-length recombinant protein of Bax (100 nM). $*p < 0.05$.

deficiency resulted in significantly increased HI brain injury at P9, partly agreeing with our previous finding that the immature brain, in contrast to the adult brain, is not protected by the CypD inhibitor CsA (Puka-Sundvall et al., 2001). CypD expression in brain mitochondria was high in both neonates and adults, making the differences in HI sensitivity unlikely to be attributable to age-dependent differences in CypD levels (Eliseev et al., 2007). Instead, the results may indicate that the CypD-dependent PTP in neonatal HI is not present to the same extent as in adult HI or that other factors regulating PTP activity are differentially expressed during development. Notably, there was a significant difference in brain injury between WT and Het at P9 (but not between Het and KO), suggesting that there is a threshold amount of CypD that is required to inhibit mitochondrial permeabilization and reduce injury *in vivo*. The fact that no difference was found between Het and KO individuals supports our choice to use only WT and KO (rather than Het) in the mechanistic characterization (Figs. 2–7).

The *in vitro* functional mitochondria experiments demonstrated that brain mitochondria from neonatal mice required higher levels of Ca^{2+} than those from adults to open the PTP. In addition, these assays showed that neonatal brain mitochondria did not respond to the PTP inhibitor CsA as efficiently as adult WT mitochondria, in keeping with the observation that CsA does not protect the brain of neonatal rats (Puka-Sundvall et al., 2001) and indicate that, after HI, PTP opening does not contribute to MP in the neonatal to the same extent as in the adult brain. Indeed, we discovered that the PTP in adult brain mitochondria displayed a lower Ca^{2+}-induced opening threshold and a higher
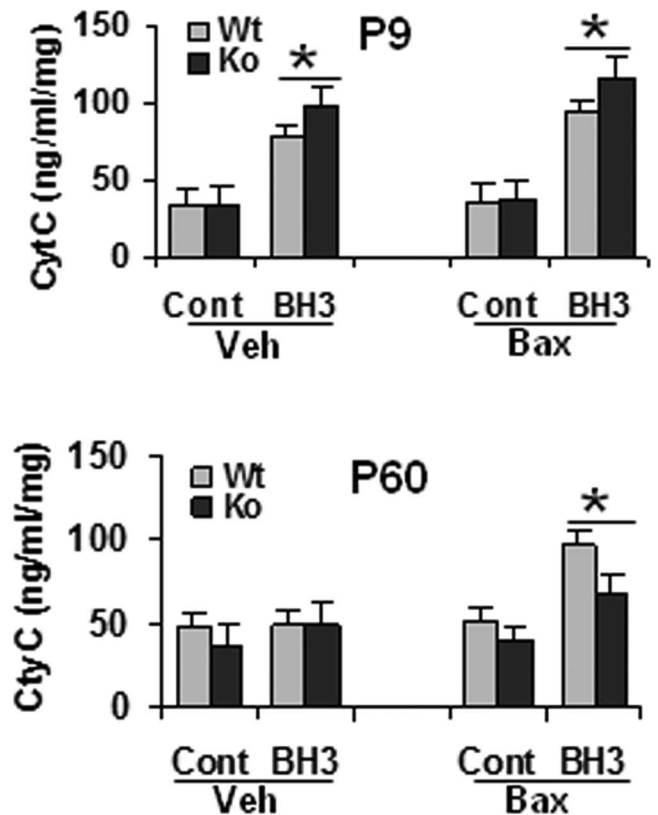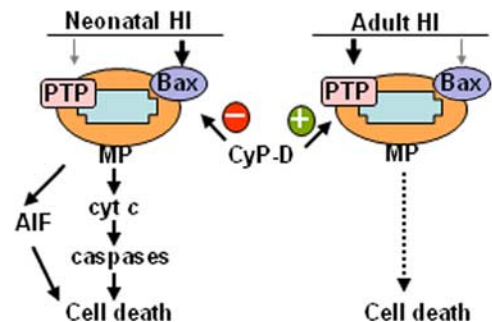

Figure 8. MP is center stage in HI brain injury at all ages, but the mechanism of MP shifts during brain development. In neonatal mice, Bax-mediated permeabilization leading to AIF- and caspase-dependent cell death, which is inhibited by CypD, predominates. In contrast, in adult animals, cell death depends on CypD-regulated and PTP-mediated mitochondrial permeabilization.

CypD dependence than in neonatal mitochondria, indicating that PTP induction only plays a critical role in ischemia-induced brain injury in the adult. Other age-dependent differences may affect MP in the complex situation of ischemia *in vivo* (Robertson et al., 2004). Spreading depression waves of Ca^{2+} uptake seem to be less prominent in the immature brain (Takita et al., 2004), in which also the anoxic depolarization with concomitant Ca^{2+} uptake is slower. Moreover, the primary energy depletion in the immature brain is much slower, with a lower accumulation of ADP/AMP and phosphate ion (Pi) and thus weaker stimuli for the opening of the PTP (Hansen and Nordstrom, 1979).

Brain injury in P9 mice was actually increased rather than

unaffected in CypD-deficient mice. In other words, Bax-dependent mechanisms of MP in the immature brain are inhibited rather than enhanced by CypD, suggesting that CypD somehow protects the immature brain. The increased brain injury in P9 KO mice was accompanied by an enhanced translocation of Bax to mitochondria compared with age-matched WT controls. *In vitro*, the BH3 peptide mimicking Bax action induced more cyt *c* release in isolated mitochondria from P9 KO than from WT mice. In contrast, similar assays of BH3 peptide-mediated cyt *c* release showed an enhanced release in WT compared with KO mice at P60, which strongly supports the *in vivo* finding. These results suggest that CypD modulates Bax activity and thereby the induction of MP and cell death. Indeed, some *in vitro* studies show that CypD overexpression desensitizes cells from apoptotic stimuli (Liu et al., 2002) and even suppresses apoptosis under some conditions (Machida et al., 2006). However, the detailed mechanisms involved need to be further investigated.

The fact that Bax inhibition substantially reduced HI injury in neonatal but not in adult mice strongly indicates that Bax-mediated MP predominates in the immature brain and that novel Bax inhibitors may have therapeutic potential (Kinnally and Antonsson, 2007). The widespread expression of Bax and its ability to heterodimerize with multiple Bcl-2 family members (Knudson et al., 1995) as well as the fact that Bax/Bak double-knock-out mice display defective apoptosis in multiple tissues (Roset et al., 2007) suggest that it may have a central role in regulating apoptosis in early development. In addition, very low levels of Bax were present in adult brain mitochondria compared with those of immature mice (Fig. 6*A*) (Vekrellis et al., 1997; Polster et al., 2003; Soane et al., 2008). *In vitro*, BH3 peptide did not induce cyt *c* release without the presence of exogenous Bax in isolated mitochondria from adult in contrast to those from neonatal mice, indicating that immature brain mitochondria are much more prone to Bax-mediated MP.

In conclusion, HI brain injury depends on Bax-mediated but not on CypD/PTP-dependent MP in the neonatal brain, whereas CypD/PTP-mediated MP is critical in the adult. Thus, during development, CypD shifts from a prosurvival molecule to a cell death enhancer after HI-induced brain injury. These data further corroborate the fundamental difference between the responses of the immature versus the adult brain to HI, which will be decisive in the choice of molecular targets for neuroprotection in the future.

References

Baines CP, Kaiser RA, Purcell NH, Blair NS, Osinska H, Hambleton MA, Brunskill EW, Sayen MR, Gottlieb RA, Dorn GW, Robbins J, Molkentin JD (2005) Loss of cyclophilin D reveals a critical role for mitochondrial permeability transition in cell death. Nature 434:658 –662.

Basso E, Fante L, Fowlkes J, Petronilli V, Forte MA, Bernardi P (2005) Properties of the permeability transition pore in mitochondria devoid of Cyclophilin D. J Biol Chem 280:18558 –18561.

Bernardi P, Krauskopf A, Basso E, Petronilli V, Blachly-Dyson E, Di Lisa F, Forte MA (2006) The mitochondrial permeability transition from in vitro artifact to disease target. FEBS J 273:2077–2099.

Cheng Y, Gidday JM, Yan Q, Shah AR, Holtzman DM (1997) Marked age-dependent neuroprotection by brain-derived neurotrophic factor against neonatal hypoxic-ischemic brain injury. Ann Neurol 41:521–529.

Du L, Bayir H, Lai Y, Zhang X, Kochanek PM, Watkins SC, Graham SH, Clark RS (2004) Innate gender-based proclivity in response to cytotoxicity and programmed cell death pathway. J Biol Chem 279:38563–38570.

Eliseev RA, Filippov G, Velos J, VanWinkle B, Goldman A, Rosier RN, Gunter TE (2007) Role of cyclophilin D in the resistance of brain mitochondria to the permeability transition. Neurobiol Aging 28:1532–1542.

Fontaine E, Eriksson O, Ichas F, Bernardi P (1998) Regulation of the permeability transition pore in skeletal muscle mitochondria. Modulation by

electron flow through the respiratory chain complex i. J Biol Chem 273:12662–12668.

Gibson ME, Han BH, Choi J, Knudson CM, Korsmeyer SJ, Parsadanian M, Holtzman DM (2001) BAX contributes to apoptotic-like death following neonatal hypoxia-ischemia: evidence for distinct apoptosis pathways. Mol Med 7:644 –655.

Grafe MR (1994) Developmental changes in the sensitivity of the neonatal rat brain to hypoxic/ischemic injury. Brain Res 653:161–166.

Gubits RM, Burke RE, Casey-McIntosh G, Bandele A, Munell F (1993) Immediate early gene induction after neonatal hypoxia-ischemia. Brain Res Mol Brain Res 18:228–238.

Hagberg H, Wilson MA, Matsushita H, Zhu C, Lange M, Gustavsson M, Poitras MF, Dawson TM, Dawson VL, Northington F, Johnston MV (2004) PARP-1 gene disruption in mice preferentially protects males from perinatal brain injury. J Neurochem 90:1068 –1075.

Hallin U, Kondo E, Ozaki Y, Hagberg H, Shibasaki F, Blomgren K (2006) Bcl-2 phosphorylation in the BH4 domain precedes caspase-3 activation and cell death after neonatal cerebral hypoxic-ischemic injury. Neurobiol Dis 21:478 –486.

Hansen AJ, Nordstrøm CH (1979) Brain extracellular potassium and energy metabolism during ischemia in juvenile rats after exposure to hypoxia for 24 h. J Neurochem 32:915–920.

Hu BR, Liu CL, Ouyang Y, Blomgren K, Siesjö BK (2000) Involvement of caspase-3 in cell death after hypoxia-ischemia declines during brain maturation. J Cereb Blood Flow Metab 20:1294 –1300.

Hurn PD, Vannucci SJ, Hagberg H (2005) Adult or perinatal brain injury: does sex matter? Stroke 36:193–195.

Johnston MV, Hagberg H (2007) Sex and the pathogenesis of cerebral palsy. Dev Med Child Neurol 49:74 –78.

Khaspekov L, Friberg H, Halestrap A, Viktorov I, Wieloch T (1999) Cyclosporin A and its nonimmunosuppressive analogue N-Me-Val-4-cyclosporin A mitigate glucose/oxygen deprivation-induced damage to rat cultured hippocampal neurons. Eur J Neurosci 11:3194 –3198.

Kinnally KW, Antonsson B (2007) A tale of two mitochondrial channels, MAC and PTP, in apoptosis. Apoptosis 12:857– 868.

Knudson CM, Tung KS, Tourtellotte WG, Brown GA, Korsmeyer SJ (1995) Bax-deficient mice with lymphoid hyperplasia and male germ cell death. Science 270:96 –99.

Kokoszka JE, Waymire KG, Levy SE, Sligh JE, Cai J, Jones DP, MacGregor GR, Wallace DC (2004) The ADP/ATP translocator is not essential for the mitochondrial permeability transition pore. Nature 427:461– 465.

Lafemina MJ, Sheldon RA, Ferriero DM (2006) Acute hypoxia-ischemia results in hydrogen peroxide accumulation in neonatal but not adult mouse brain. Pediatr Res 59:680 –683.

Liu Y, Silverstein FS, Skoff R, Barks JD (2002) Hypoxic-ischemic oligodendroglial injury in neonatal rat brain. Pediatr Res 51:25–33.

Machida K, Ohta Y, Osada H (2006) Suppression of apoptosis by cyclophilin D via stabilization of hexokinase II mitochondrial binding in cancer cells. J Biol Chem 281:14314 –14320.

Matsumoto S, Friberg H, Ferrand-Drake M, Wieloch T (1999) Blockade of the mitochondrial permeability transition pore diminishes infarct size in the rat after transient middle cerebral artery occlusion. J Cereb Blood Flow Metab 19:736 –741.

Nakagawa T, Shimizu S, Watanabe T, Yamaguchi O, Otsu K, Yamagata H, Inohara H, Kubo T, Tsujimoto Y (2005) Cyclophilin D-dependent mitochondrial permeability transition regulates some necrotic but not apoptotic cell death. Nature 434:652– 658.

Ness JM, Harvey CA, Strasser A, Bouillet P, Klocke BJ, Roth KA (2006) Selective involvement of BH3-only Bcl-2 family members Bim and Bad in neonatal hypoxia-ischemia. Brain Res 1099:150 –159.

Nijboer CH, Groenendaal F, Kavelaars A, Hagberg HH, van Bel F, Heijnen CJ (2007) Gender-specific neuroprotection by 2-iminobiotin after hypoxia-ischemia in the neonatal rat via a nitric oxide independent pathway. J Cereb Blood Flow Metab 27:282–292.

Northington FJ, Ferriero DM, Flock DL, Martin LJ (2001) Delayed neurodegeneration in neonatal rat thalamus after hypoxia-ischemia is apoptosis. J Neurosci 21:1931–1938.

Parsadanian AS, Cheng Y, Keller-Peck CR, Holtzman DM, Snider WD (1998) Bcl-xL is an antiapoptotic regulator for postnatal CNS neurons. J Neurosci 18:1009 –1019.

Polster BM, Robertson CL, Bucci CJ, Suzuki M, Fiskum G (2003) Postnatal brain development and neural cell differentiation modulate mitochon-

drial Bax and BH3 peptide-induced cytochrome c release. Cell Death Differ 10:365–370.

Puka-Sundvall M, Gilland E, Hagberg H (2001) Cerebral hypoxia-ischemia in immature rats: involvement of mitochondrial permeability transition? Dev Neurosci 23:192–197.

Rasola A, Bernardi P (2007) The mitochondrial permeability transition pore and its involvement in cell death and in disease pathogenesis. Apoptosis 12:815–833.

Renolleau S, Fau S, Goyenvalle C, Joly LM, Chauvier D, Jacotot E, Mariani J, Charriaut-Marlangue C (2007) Specific caspase inhibitor Q-VD-OPh prevents neonatal stroke in P7 rat: a role for gender. J Neurochem 100:1062–1071.

Renolleau S, Fau S, Charriaut-Marlangue C (2008) Gender-related differences in apoptotic pathways after neonatal cerebral ischemia. Neuroscientist 14:46–52.

Robertson CL, Bucci CJ, Fiskum G (2004) Mitochondrial response to calcium in the developing brain. Brain Res Dev Brain Res 151:141–148.

Roset R, Ortet L, Gil-Gomez G (2007) Role of Bcl-2 family members on apoptosis: what we have learned from knock-out mice. Front Biosci 12:4722–4730.

Sakata A, Tamai I, Kawazu K, Deguchi Y, Ohnishi T, Saheki A, Tsuji A (1994) In vivo evidence for ATP-dependent and P-glycoprotein-mediated transport of cyclosporin A at the blood-brain barrier. Biochem Pharmacol 48:1989–1992.

Schinzel AC, Takeuchi O, Huang Z, Fisher JK, Zhou Z, Rubens J, Hetz C, Danial NN, Moskowitz MA, Korsmeyer SJ (2005) Cyclophilin D is a component of mitochondrial permeability transition and mediates neuronal cell death after focal cerebral ischemia. Proc Natl Acad Sci U S A 102:12005–12010.

Scorrano L, Nicolli A, Basso E, Petronilli V, Bernardi P (1997) Two modes of activation of the permeability transition pore: the role of mitochondrial cyclophilin. Mol Cell Biochem 174:181–184.

Soane L, Siegel ZT, Schuh RA, Fiskum G (2008) Postnatal developmental regulation of Bcl-2 family proteins in brain mitochondria. J Neurosci Res 86:1267–1276.

Takita M, Puka-Sundvall M, Miyakawa A, Hagberg H (2004) In vivo calcium imaging of cerebral cortex in hypoxia-ischemia followed by developmental stage-specific injury in rats. Neurosci Res 48:169–173.

Uchino H, Elmér E, Uchino K, Lindvall O, Siesjö BK (1995) Cyclosporin A dramatically ameliorates CA1 hippocampal damage following transient forebrain ischaemia in the rat. Acta Physiol Scand 155:469–471.

Vannucci SJ, Willing LB, Goto S, Alkayed NJ, Brucklacher RM, Wood TL, Towfighi J, Hurn PD, Simpson IA (2001) Experimental stroke in the female diabetic, db/db, mouse. J Cereb Blood Flow Metab 21:52–60.

Vekrellis K, McCarthy MJ, Watson A, Whitfield J, Rubin LL, Ham J (1997) Bax promotes neuronal cell death and is downregulated during the development of the nervous system. Development 124:1239–1249.

Wang X, Karlsson JO, Zhu C, Bahr BA, Hagberg H, Blomgren K (2001) Caspase-3 activation after neonatal rat cerebral hypoxia-ischemia. Biol Neonate 79:172–179.

Wang X, Zhu C, Qiu L, Hagberg H, Sandberg M, Blomgren K (2003) Activation of ERK1/2 after neonatal rat cerebral hypoxia-ischaemia. J Neurochem 86:351–362.

Wang X, Zhu C, Wang X, Gerwien JG, Schrattenholz A, Sandberg M, Leist M, Blomgren K (2004a) The nonerythropoietic asialoerythropoietin protects against neonatal hypoxia-ischemia as potently as erythropoietin. J Neurochem 91:900–910.

Wang X, Zhu C, Wang X, Hagberg H, Korhonen L, Sandberg M, Lindholm D, Blomgren K (2004b) X-linked inhibitor of apoptosis (XIAP) protein protects against caspase activation and tissue loss after neonatal hypoxia-ischemia. Neurobiol Dis 16:179–189.

Wang X, Hagberg H, Mallard C, Zhu C, Hedtjärn M, Tiger CF, Eriksson K, Rosen A, Jacobsson B (2006) Disruption of interleukin-18, but not interleukin-1, increases vulnerability to preterm delivery and fetal mortality after intrauterine inflammation. Am J Pathol 169:967–976.

Yager JY, Heitjan DF, Towfighi J, Vannucci RC (1992) Effect of insulin-induced and fasting hypoglycemia on perinatal hypoxic-ischemic brain damage. Pediatr Res 31:138–142.

Zamzami N, Larochette N, Kroemer G (2005) Mitochondrial permeability transition in apoptosis and necrosis. Cell Death Differ 12 [Suppl 2]:1478–1480.

Zhu C, Qiu L, Wang X, Hallin U, Candé C, Kroemer G, Hagberg H, Blomgren K (2003) Involvement of apoptosis-inducing factor in neuronal death after hypoxia-ischemia in the neonatal rat brain. J Neurochem 86:306–317.

Zhu C, Wang X, Xu F, Bahr BA, Shibata M, Uchiyama Y, Hagberg H, Blomgren K (2005) The influence of age on apoptotic and other mechanisms of cell death after cerebral hypoxia-ischemia. Cell Death Differ 12:162–176.

Zhu C, Xu F, Wang X, Shibata M, Uchiyama Y, Blomgren K, Hagberg H (2006) Different apoptotic mechanisms are activated in male and female brains after neonatal hypoxia-ischaemia. J Neurochem 96:1016–1027.

Zoratti M, Szabò I, De Marchi U (2005) Mitochondrial permeability transitions: how many doors to the house? Biochim Biophys Acta 1706:40–52.